ADVANCES MODELLING AND SIMULATION OF INDUSTRIAL BOILERS

M. Sadrameli and K. A. Khazaee

Department of Chemical Engineering
Tarbiat Modarres University
Tehran, Iran

Abstract This paper presents some of the results of the simulation in the radiation section of an industrial boiler using an advanced mathematical model. Calculations are described for the flow, heat transfer, and chemical reaction processes occurring within a gas-fired cylindrical furnace. The calculation procedure is a two dimensional one in which the main hydrodynamic variables are the velocity and stream functions. The turbulence formulae are used for this purpose. Mass transfer and chemical reactions are calculated from the model which assumes a single-step chemical reaction. Heat transfer is determined by the solution of differential equations for the specific enthalpy, and for the radiative fluxes for each of the co-ordinate directions. The resulting system of coupled, non linear, elliptic, partial differential equations gives the velocity and temperature gradients inside the furnace. The results are compared with those reported in the literature and good agreements between them were found.

Key Words Boilers, Heat Transfer, Modelling, Simulation

چکیده دراین مقاله نتایج شبیه سازی بخش تشعشع دیگهای بخار صنعتی توسط مدلسازی ریاضی پیشرفته ارائه گردیده است. محاسبات انجام شده جهت انتقال حرارت، مقدار جریان سیال، واکنش شیمیایی اجزاء در فرآیند احتراق در کوره های استوانه ای شکل با سوخت گازی می باشد، روش محاسبه با استفاده از مدلهای دو بعدی بوده که درآن متغیرهای هیدرودینامیکی شامل توابع سرعت و جریان می باشند. جهت محاسبات از فرمول تلاطم استفاده گردیده است. انتقال جرم و واکنشهای شیمیایی توسط مدلی محاسبه گردیده که در آن فرض شیمیایی یک مرحله ای منظور گردیده است. انتقال حرارت توسط حل معادلات دیفرانسیل شامل معادلات انتالپی مخصوص، و شار تشعشعی برای هرجهت مختصات صورت گرفته است. معادلات دیفرانسیل شامل سری معادلات غیرخطی، بیضوی و معادلات جزئی در گرادیان سرعت و درجه حرارت در کوره می باشد. نتایج بدست آمده از حل معادلات دیفرانسیل با نتایج تجربی ارائه شده در منابع مقایسه و نشاندهندهٔ دقت محاسبات در مدل می باشد.

INTRODUCTION

The design of furnaces would be greatly facilitated by a procedure for calculating wall heat transfer and local flow properties as a function of furnace geometry and burner conditions. Such a calculation procedure allows the influences of air/fuel ratio, mass flowrates, burner-exit geometry and enclosure dimensions on the distribution of heat flux to be determined; the regions of unburned fuel could be located and reduced; and regions of high temperature and of consequent NO_x formation could be avoided.

The main purpose of this project was to test one of the particular calculation procedures, based on the solution of the conservation equations in differential time averaged form. This is done by the comparison of the results with experimental data. Since no experimental data are available in the literature for the boiler operation, the success of the calculation procedure is checked by the comparisons of the calculated results and simulation results presented in [1].

1. MATHEMATICAL MODELLING

1.1 Governing Differential Equaitons:

The geometry of the furnace arrangements, shown in Figure 1, is encountered in flows with substantial regions of recirculation. The equations used to represent conservation of the flow properties were, therefore, elliptic in form and were expressed in cylindrical coordinates. The general form of the equation is [1]:

$$a_\varphi \left\{ \frac{\partial}{\partial z}\left(\varphi \frac{\partial \psi}{\partial r}\right) - \frac{\partial}{\partial r}\left(\varphi \frac{\partial \psi}{\partial z}\right) \right\} - \frac{\partial}{\partial z}\left\{ b_\varphi . r. \frac{\partial (C_\varphi . \varphi)}{\partial z} \right\}$$

$$- \frac{\partial}{\partial r}\left\{ b_\varphi . r. \partial \frac{(C_\varphi . \varphi)}{\partial r} \right\} + r.d_\varphi = 0 \qquad (1)$$

with the corresponding values of a_ϕ, b_ϕ, c_ϕ and d_ϕ indicated in Table 1. In addition, equations presented in Table 1, are derived from the formulation of the conservation of mass, momentum, chemical species, and energy. The equations for the physical processes such as turbulent transport and radiation are also added to the system of equations. The need to introduce additional physical models arises because many of the processes that occur in the furnace are far too complex to be handled at a fundamental level of calculation.

1.1.1 *Conservation Equations*

It is assumed that no external body forces act on the system; that species diffusion follows Fick's law; that the Lewis number for each chemical species is unity; that kinetic heating terms in the energy equation are negligible; and that the gas follows the ideal gas equation of state. With these assumptions, the equations for conservation of mass, momentum, chemical species, and energy may be written as illustrated in Table 1. The instantaneous equations are transformed to yield equations for the time-average variables using a procedure known as Reynolds decomposition [2].

1.1.2 *Turbulence Models*

In the momentum, chemical species and energy

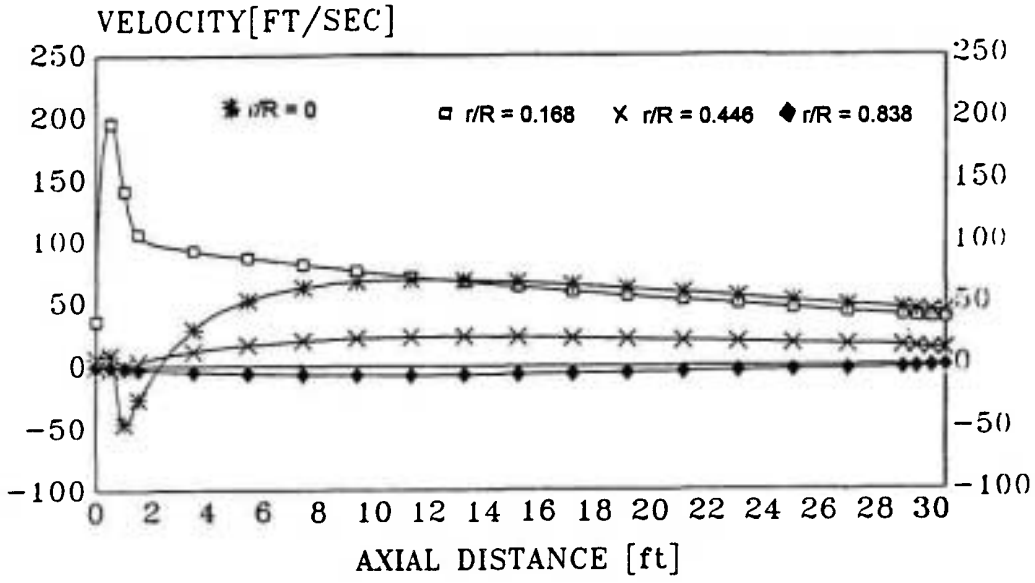

Figure 1. Axial velocity profiles at different r/R ratios.

TABLE 1. Conservation Equations Corresponding to Equation 1.

φ	a_φ	b_φ	c_φ	d_r
m_{fu}	1	$\frac{\mu_{eff}}{\sigma_{fu\text{-}eff}}$	1	$-R_{fu}$
h	1	$\frac{\mu_{eff}}{\sigma_{h\text{-}eff}}$	1	$-S_R$
rV_3	1	$\mu_{eff} r^2$	$\frac{1}{r^2}$	0
$\frac{\omega}{r}$	r^2	r^2	μ_{eff}	$\frac{-\partial}{\partial z}(\rho V_3^2) - \frac{\rho}{l_1 l_2}[\frac{\partial}{\partial \zeta_1}(\frac{V_1^2 + V_2^2}{2}) - \frac{\partial \rho}{\partial \zeta_2}$ $- \frac{-\partial}{\partial \zeta_2}(\frac{V_1^2 + V_2^2}{2}) \cdot \frac{\partial \rho}{\partial \zeta_1}]$
ψ	0	$\frac{1}{\rho r^2}$	1	$-\frac{\omega}{r}$
K	1	$\frac{\mu_{eff}}{\sigma_{keff}}$	1	$-(S_k - \rho\epsilon)$
ϵ	1	$\frac{\mu_{eff}}{\sigma_{\epsilon eff}}$	1	$-\frac{\epsilon}{k}(C_1 S_k - C_2 \rho\epsilon)$
f	1	$\frac{\mu_{eff}}{\sigma_{f\text{-}eff}}$	1	0
g	1	$\frac{\mu_{eff}}{\sigma_{g\text{-}eff}}$	1	$-(C_{g1} G_{g1} - C_{g2} \rho \frac{\epsilon}{K} g)$

conservation equation; turbulent transport of momentum, mass and energy may be modelled using the Boussinesq approximation to relate the turbulent fluxes to mean flow property gradients via turbulent fluxes, according to Newton, Fick and Fourier laws. Since the transport of species, enthalpy, and momentum occur by similar turbulent exchange processes, the turbulent exchange coefficients for species and enthalpy can be assumed proportional to the turbulent viscosity. In summary the main objective of the present model is to evaluate the transport property by calculating the turbulent viscosity, and this will be achieved by presentation of a "two-equation" or "K-ε" model [3]. Here for the sake of economy and lack of enough boundary conditions for the model, another formulae is used [4] as:

$$\mu_{eff} = K_1 D^{2/3} W^{1/3} \rho^{2/3} (m_F^o V_F^2 + m_o^o V_o^2)^{1/3} \quad (2)$$

further details of the mathematical models may be found in References 2, 3 and 5.

1.1.3 *Turbulent Combustion Models*

The equations for the species concentration and the species concentration fluctuation represent the combustion processes and will be referred to the combustion model. There are three main combustion models [6], but for the sake of accuracy, one of the models is considered here, in which the fuel and the oxidant are assumed to flow through separate inlet streams, one step reaction, with fuel and oxidant unable to coexist at the same location, and with the assumption of infinitely fast chemistry (physically controlled). The only species equation to be solved is

the mixture fraction f. By evaluating f, the instantaneous species mass fraction is completely determined. It should be mentioned that, the other two combustion and two-equation models discussed previously in Section 1.1.2 can be solved with the present simulation method. Further details of these models may be found in References 2, 5 and 6.

1.1.4 *Radiation Models*

Thermal radiation enters as a source term in the enthalpy equation. For the evaluation of this term, radiation models are introduced. Thermal radiation is normally governed by an increasingly complex procedure, involving a coupling of the integral equations of the zone method to the differential equation of the flow, chemical reaction, and heat transfer. A simpler method is to replace the integro-differential equation by a system of differential equations using a flux approximation method [7].

The advantages which this transformation brings are two fold; first, the differential equations can be solved by standard finite-difference techniques; and second, the finite-difference equations are of the space "sparse-matrix" kind, where in a zone temperature, it is linked only to its immediate neighbours. Corresponding to one, two and three dimensional co-ordinate system, there are two, four and six flux models respectively. In the present research, a four flux model is used; therefore, equations of model are written for the rate of change of positive radiation fluxes I and J in the positive and negative co-ordinate directions. In the absence of scattering, they are, for the axial direction [7]:

$$\frac{dI_z}{dz} = -a \cdot I_z + a \cdot E \tag{3}$$

$$\frac{dJ_z}{dz} = -a \cdot I_z + a \cdot E \tag{4}$$

and for the radial direction:

$$\frac{d(rI_r)}{dr} = [-a \cdot I_r + (J_r / r) + \dot{a} \cdot E \tag{5}$$

$$\frac{d(rJ_r)}{dr} = [-a \cdot J_r + (J_r / r) + a \cdot E \tag{6}$$

The working equations may be resulted with the combinatin of each pair of first-order flux equations to yield a single second-order equation [7]:

$$\frac{d}{dz} = \left[\Gamma_z \frac{dF_z}{dz}\right] + a(E - F_z) = 0 \tag{7}$$

$$\frac{1}{r}\frac{d}{dz} = \left[\Gamma_r \cdot r \frac{dF_r}{dr}\right] + a(E - F_r) = 0 \tag{8}$$

These are the working equations, which cast into finite-difference form; and the calculation of the radiation fluxes was embedded in the iteration cycle employed for the other variables. Further details of this model can be found in Reference 7.

1.1.5 *Boundary Conditions*

The elliptic form of the conservation equations represented by Equation 1 necessitates the specification of boundary conditions, for each dependent variable, at each surface of the solution domain. This domain was a symmetrical half-section of the furnace and symmetry condition was, therefore, imposed on the axis. The solid wall boundary, inlet and outlet conditions can be found in References 5, 6 and 7.

2. NUMERICAL SOLUTIONS OF THE MODEL

The differential equations represented by Equation 1 and Table 1 were expressed in the finite difference form as presented in Reference 5 and solved by the algorithm of that reference. The present calculations were performed with a grid composed of 21-21 nodes

and allowed the solution of six equations (corresponding to $\omega/r, \psi, f, h, F_z, F_r$) in approximately 2.5 minutes CPU time on an "IBM compatible 486 DX33 MHZ" machine. The spacing between the nodes, was adjusted to concentrate the nodes in the regions of steep variations. A full description of the method is beyond the scope of this paper. For the details of the numerical solutions the reader is referred to References 5, 6 and 7.

RESULTS

The simulation results presented in this section, correspond to a non-swirling flame and combusting flow in a furnace with a single burner as discussed in Reference 1. The simulation results can be divided into seven parts as follows:

a) Distributions of the stream function and velocities (axial and radial)

b) Distribution of the mixture fraction and mass fractions of fuel, air and products

c) Distribution of enthalpy and therefore gas, tube skin and refractory temperatures

d) Distribution of radiation heat flux for the flow and total heat flux on the tubes

e) Heat absorbed by the tubes and therefore efficiency of the furnace

f) Prediction of the flame length and influences of variation of furnace parameters such as; air/fuel ratio, mass flow rates, burner-exist geometry and enclosure dimension of heat flux and the furnace efficiency

g) Distribution of density, viscosity and other physical properties

Full details of the results can be obtained from Reference 5 of the results are presented here.

Figures 1 to 3 illustrate the axial and radial velocities and fuel mass fraction profiles versus axial distance at different radial cross sections. Figure 4 displays the distribution of the net radiation heat flux calculated by the radiation model in the radial direction. Figures 5 to 9 represent the gas temperature distribution which are compared with the results of the zone method discussed in Reference

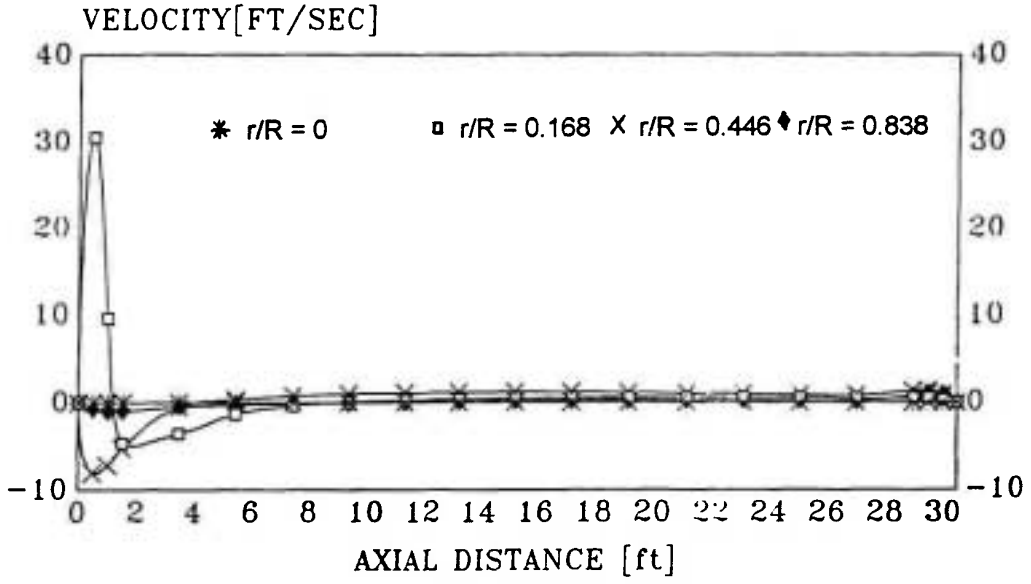

Figure 2. Radial velocity profiles at different r/R ratios.

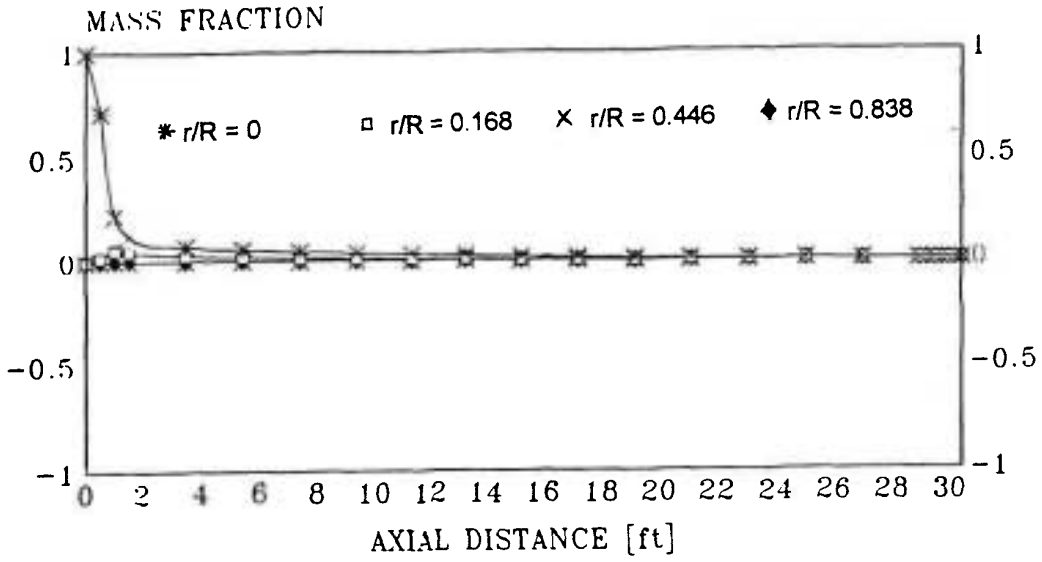

Figure 3. Fuel mass fraction profiles.

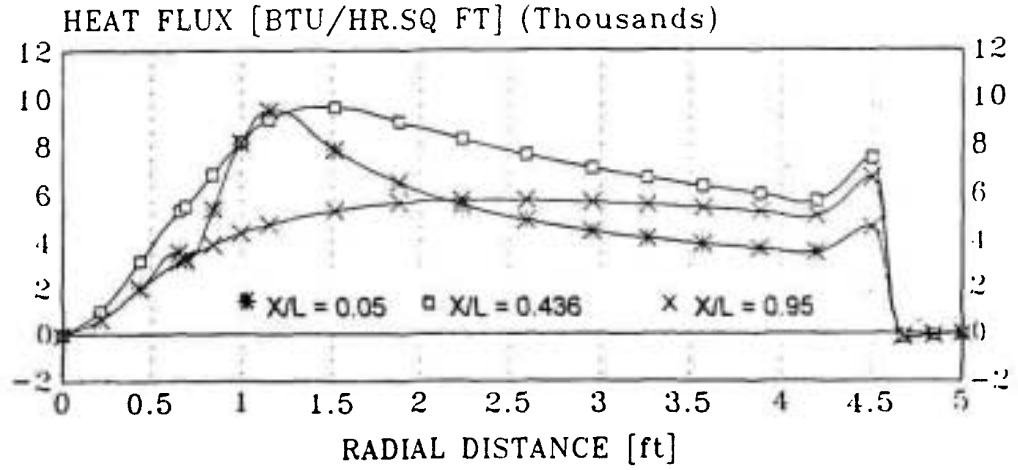

Figure 4. Radial radiation heat flux at different tube length.

1; tube skin temperature and total heat flux distributions for the present work and the results of the zone method. A representative comparison of the furnace simulation results and the results of the zone method is shown in Figure 10. Figure 11 illustrates the simulated efficiencies against the temperature of the inlet air for different values of excess air.

4. DISCUSSION

The comparison presented in section 3 shows that the results obtained with the present model are in good agreement with the results of the zone model. For the results illustrated in Figures 1 to 4, no experimental data are available for the comparison; but it is unsaid

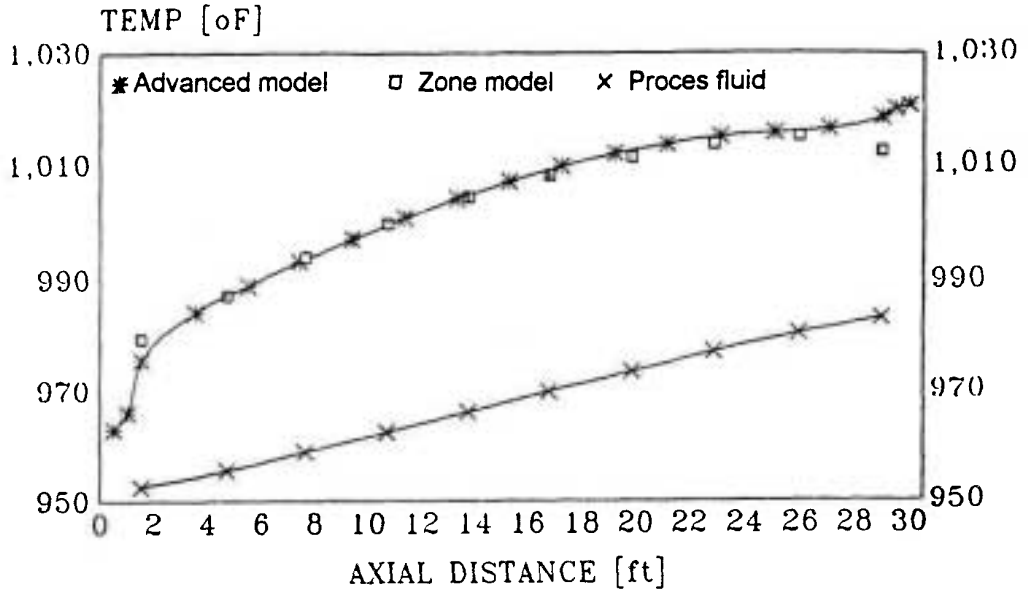

Figure 5. Comparison of the tube wall temperature pofiles.

that, these results are in good agreement with the results of the zone method reported in References 1, 6, and 7. As can be seen from Figures 1 and 2, the distribution of the mean axial and radial velocities are very complicated.

The corresponding fluctuations of the velocity are comparatively large close to the burner (reaction zone) and tends to a uniform and lower value at downstream locations. Recirculation zones which correspond to the negative values of velocities, are related to the mean temperature and correspondingly low values of density used in the solution of the momentum equation for the hotter regions of the flow. In the near wall regions, due to the lower values of the mean temperature and the correspondingly high values of density, and therefore more effects of the gravity force, the flow comes down. This happens as the results of the convection heat transfer. As can be seen from Figure 3, all of the combustion take place in the central row of the combustion takes place in the central row of the furnace and is distributed according to the flow pattern. This result is in a good agreement with the results reported in Reference 2.

As illustrated in Figure 4, in the centre line and at the wall surfaces of the furnance, zero values of net radiation heat flux, correspond to the axial symmetry and also adiabatic boundary condition respectively. The maximum values for the net radiation heat flux corresponds to the reaction zones in which the fuel-air mixture is stochiometric and therefore results the maximum temperature.

Figures 5 to 7 show that the corresponding fluctuation in temperature is comparatively large close to the burner (reaction zone) and tends to a uniform and lower values at the down stream locations. The location of the maximum temperature fluctuation corresponds approximately to the end part of the luminous flame zones. The maximum discrepancies between the present model and the zone model are the reaction zones according to the combustion model considered. As can be seen from Figures 8 to 10, the two sets of data are in good agreement. It is interesting to note from Figure 9 that, 96% of the total heat flux on the tubes are related to the radiation and only 4%

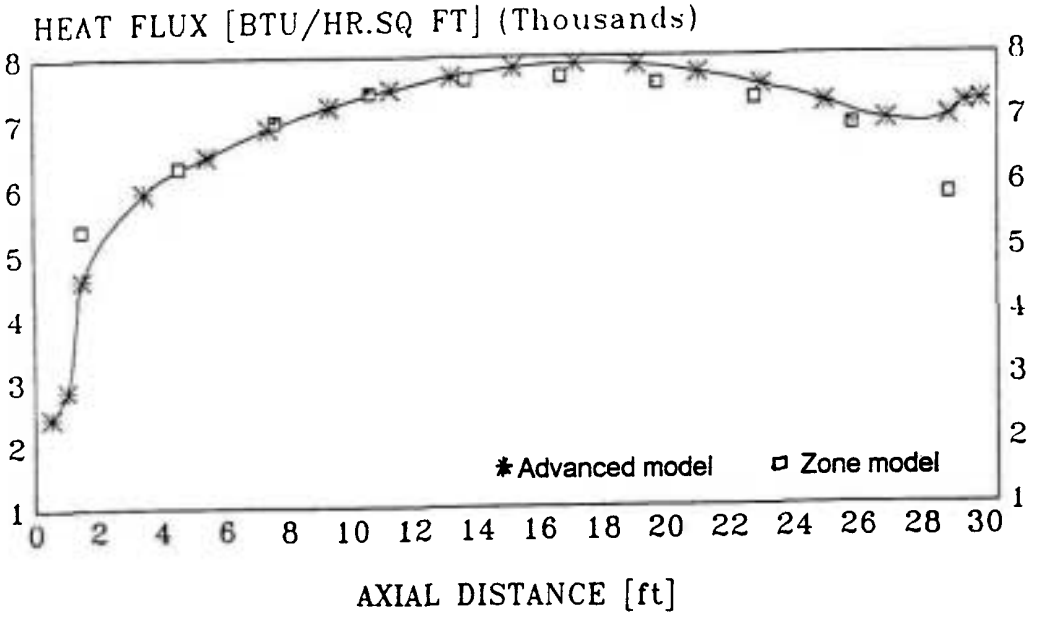

Figure 6. Comparison of the tube wall heat flux profiles.

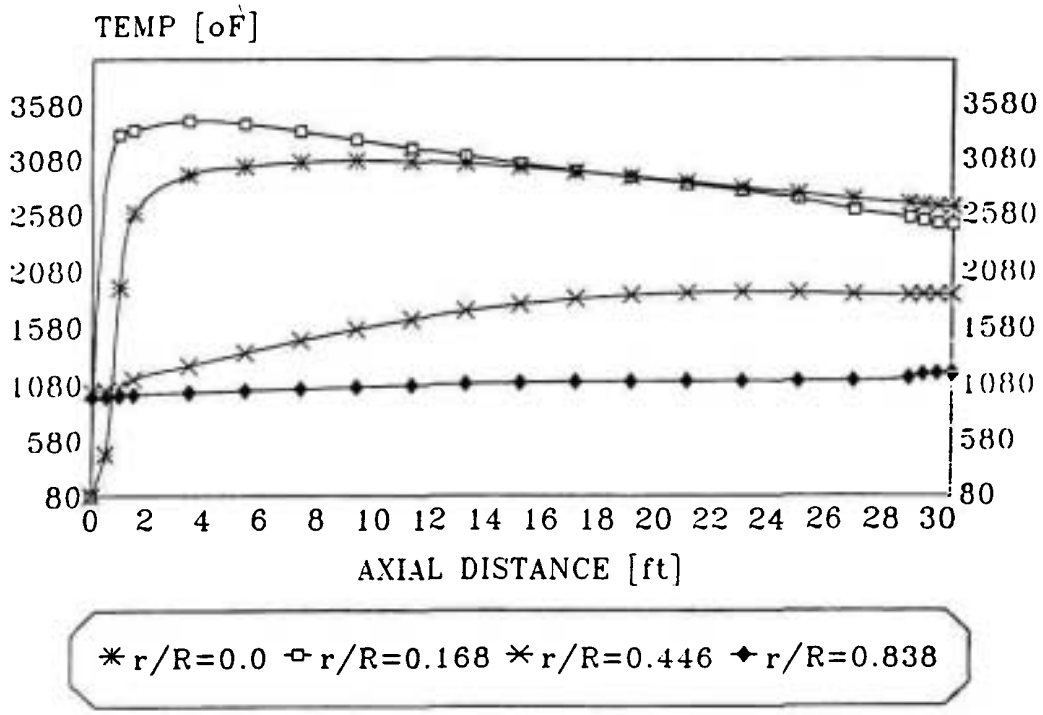

Figure 7. Axial gas temperature profiles at different r/R ratios.

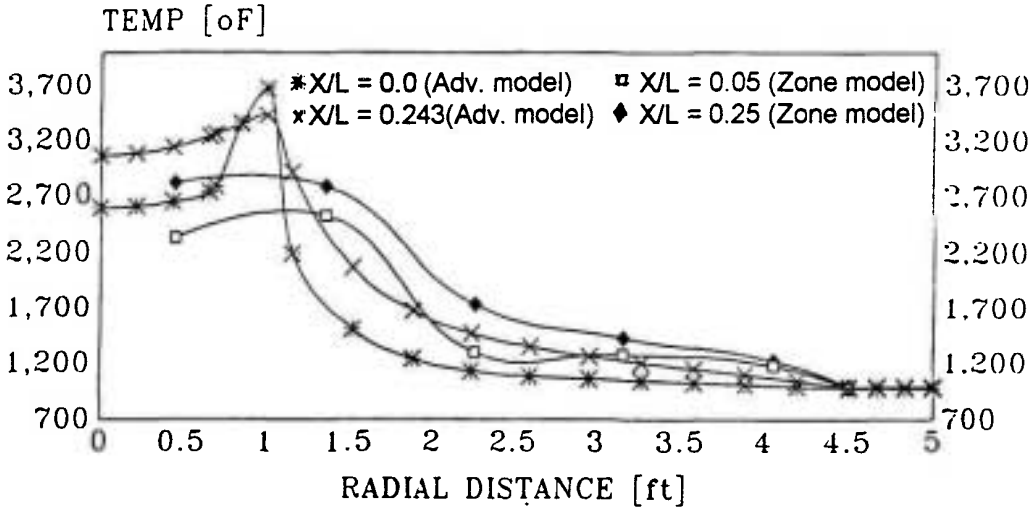

Figure 8. Radial gas temperature profile at different length of tube.

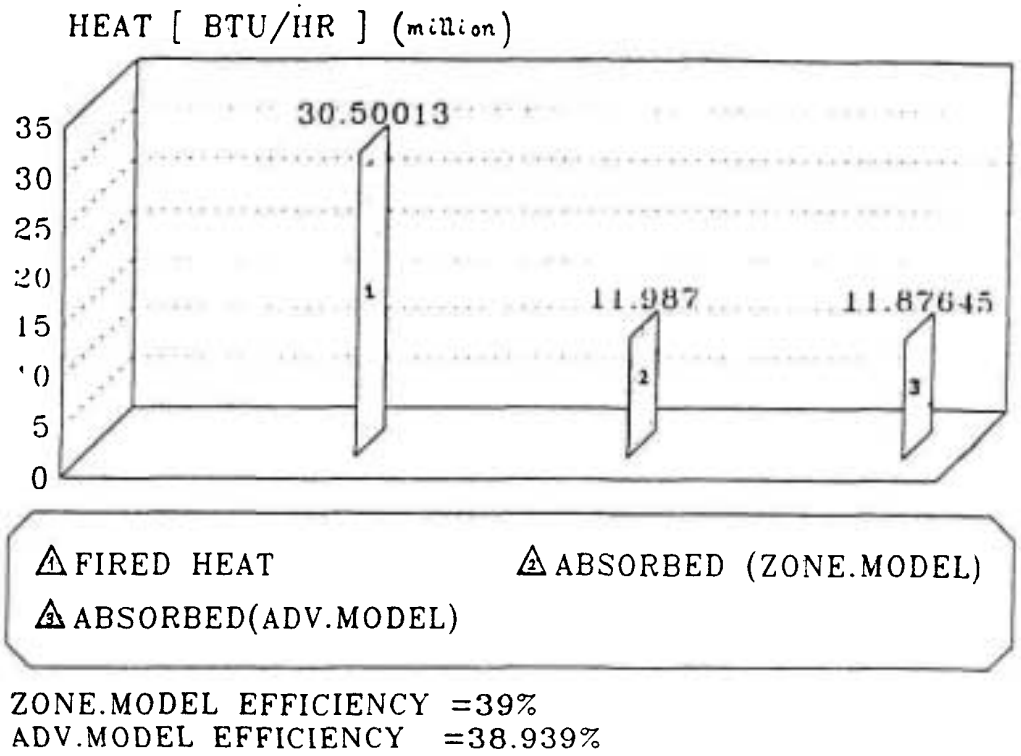

Figure 9. Boiler performance.

are from convection heat transfer. This is also validated when compared with the results of Reference 1. According to Figure 11, the furnace efficiency increases with decreasing excess air and increasing air inlet temperature. In other words, if the temperature of the inlet air is increased by 20°F, the efficiency

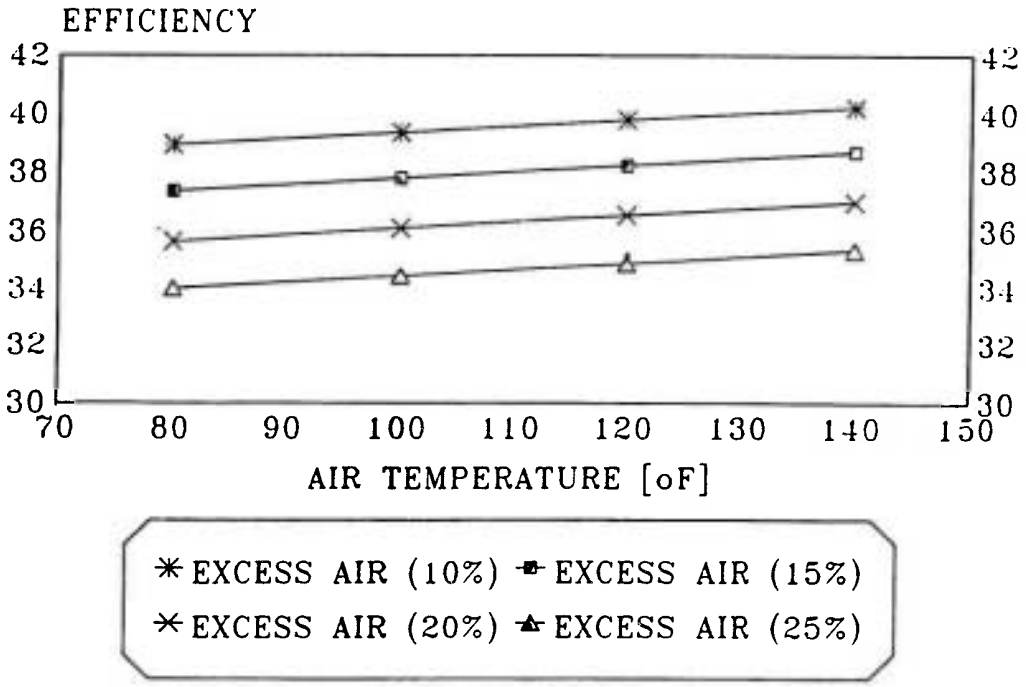

Figure 10. Effect of excess air on the boiler efficiency.

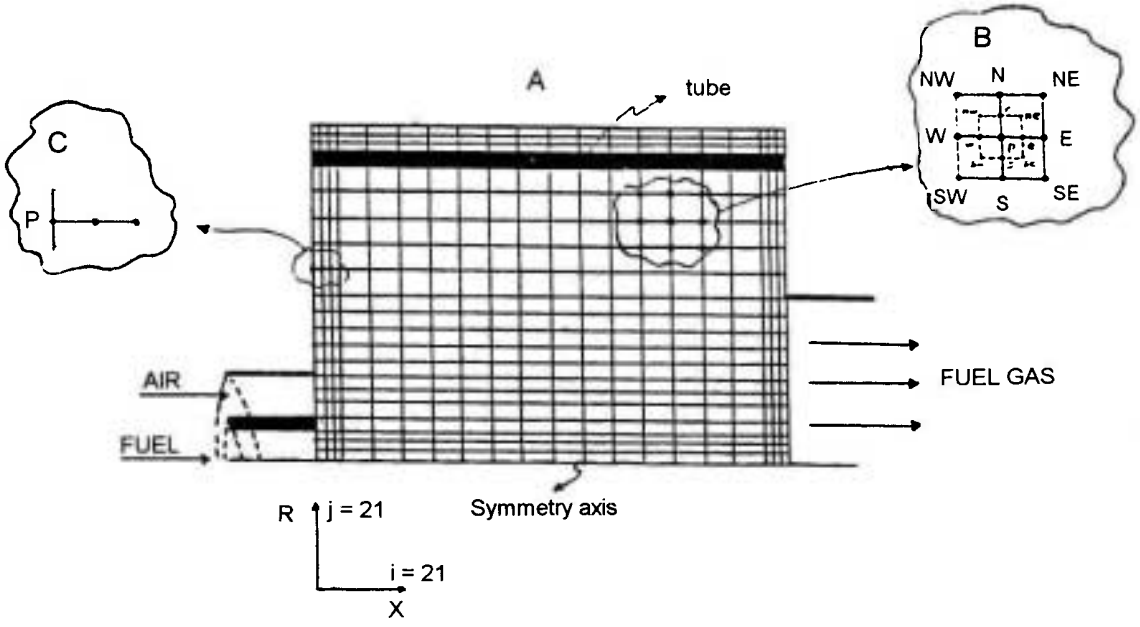

A: Furnace and grid arrangement
B: Finite difference grid of interior nodes
C: Finite difference grid of boundary nodes

Figure 11. Boiler grid arrangement.

increase is 0.5%, and this is proved by the experimental data.

5. CONCLUSION

The comparison presented in Section 4 shows that the results obtained by the present model are in a good agreement with the results of the zone method used for analysis of the industrial furnaces and boilers. This is sufficient to justify the calculations for many engineering purposes. In addition it may be concluded that the present mathematical model including turbulence model and four flux radiation model is able to represent the furnace flows of the type described in Reference 1, and that the accuracy and fluxibility of the present model for the simulation of the furnaces is higher than that of the zone model. This is because of the limitation of the zone method which provides only a solution for the radiation component of the overall furnace heat transfer problem.

NOMENCLATURE

a	flux-model absorption coefficient
c_1, c_2	constants in turbulence model
c_{g1}, c_{g2}	constants in combustion model
D	furnace diameter
E	black body emissive power, σT^4
f	mixture fraction
F	radiation flux sum, (I+J)/2
g	square of the fluctuation of concentration
G_{g1}	correlation related to g-equation
h	stagnation enthalpy
I	positive radiation flux in the positive co-ordinate direction
I	stoichiometric mass of air per unit mass of fuel
J	positive radiation flux in the negative co-ordinate direction
k	kinetic energy of turbulence
k_1	constant
m	mass fraction
m°	mass flow rate
r	radial distance from axis of symmetry
R_{fu}	rate of chemical reaction
S_k	correlation related to k-equation
S_R	source of sink of energy per unit volume and time associated with radiation
T	absolute temperature
V_1, V_2	fluid mean velocity in the axial and radial direction respectively
V_3	normal tangential velocity
W	furnace length
Z	axial co-ordinate along the furnace

Greek Symbols

Γ	exchange coefficient
μ_{eff}	effective viscosity
μ	molecular viscosity
μ_t	turbulent viscosity
ρ	density
σ	Stefan-Boltzmann constant
σ_ϕ	Schmidt and Prandtl number for any variable ϕ
ε	dissipation of energy
Φ	dependent variable
ϕ	general dependent variable
ψ	stream function
ω	vorticity

Subscripts

O	oxidant stream
F	fuel stream
fu	fuel
r	radial direction
Z	axial direction

REFERENCES

1. R. Nogay, "Better Design Methods for Fired Heaters",

Hydrocarbon Processing, (Nov. 1985).

2. J. S. Truelove, "Furnaces and Combustion Chambers", Heat Exchanger Design Handbook, Sec. 3.11, (1983).
3. B. E. Launder and D. B. Spalding, "Mathematical Models of Turbulence", Academic Press, New York, (1972).
4. W. M. Pun and D. B. Spalding, "A Procedure for Predicting the Velocity and Temperature Distribution in a Confined, Steady, Turbulent, Gaseous, Dffusion Flame", Imperial College, Mech. Eng. Dept. Rep. SF/TN/11, (1967).
5. K. Abbasi-Khazaee, "Advanced Modelling and Simulation of Industrial Boilers", MSc Thesis, Tarbiat Modarres University, Iran, (1995).
6. E. E. Khalil and J. H. Whitlaw, "The Calculation of Local Flow Properties in Two Dimensional Furnaces", Imperial College, Mech. Eng. Dept. Rep. HTS/74/38, (1975).
7. A. D. Gosmann and F. C. Lockwood, "Incorporation of Flux Model for Radiation into a Finite Difference Procedure for Furnace Calculation", Proc. 14th Int. Symp. Comb., Combustion Inst., USA, (1972), 661-671.